# Template polymerization synthesis of hydrogel and silica composite for sorption of some rare earth elements

**Article** *in* Journal of Colloid and Interface Science · October 2015

DOI: 10.1016/j.jcis.2015.06.020

CITATIONS
4

READS
190

**5 authors**, including:

Emad H Borai
Egyptian Atomic Energy Authority
**61** PUBLICATIONS **511** CITATIONS
SEE PROFILE

Mahmoud Goneam Hamed
Egyptian Atomic Energy Authority
**2** PUBLICATIONS **5** CITATIONS
SEE PROFILE

A. M. El-kamash
Egyptian Atomic Energy Authority
**48** PUBLICATIONS **845** CITATIONS
SEE PROFILE

Gamal El-Sayed
Benha University
**52** PUBLICATIONS **493** CITATIONS
SEE PROFILE

Journal of Colloid and Interface Science 456 (2015) 228–240

Contents lists available at ScienceDirect

Journal of Colloid and Interface Science

journal homepage: www.elsevier.com/locate/jcis

# Template polymerization synthesis of hydrogel and silica composite for sorption of some rare earth elements

E.H. Borai [a], M.G. Hamed [a,*], A.M. El-kamash [a], T. Siyam [a], G.O. El-Sayed [b]

[a] Hot Laboratories Center, Atomic Energy Authority, 13759, Egypt
[b] Chemistry Department, Benha University, Egypt

## GRAPHICAL ABSTRACT

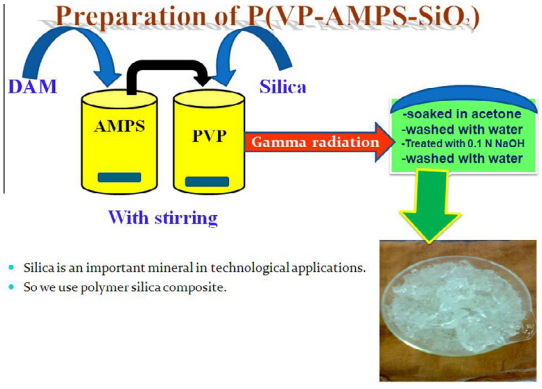


## ARTICLE INFO

*Article history:*
Received 6 April 2015
Accepted 11 June 2015
Available online 17 June 2015

*Keywords:*
Polymer
Adsorption
Rare earth elements

## ABSTRACT

New sorbents containing 2-acrylamido 2-methyl propane sulphonic acid monomer onto poly(vinyl pyrilidone) P(VP-AMPS) hydrogel and P(VP-AMPS-$SiO_2$) composite have been synthesized by radiation template polymerization. The effect of absorbed dose rate (kGy), crosslinker concentration and polymer/-monomer ratio on the degree of template polymerization of P(VP-AMPS) hydrogel was studied. The degree of polymerization was evaluated by the calculated percent conversion and swelling degree. The maximum capacity of P(VP-AMPS) hydrogel toward $Cu^{+2}$ metal ion found to be 91 mg/gm. The polymeric composite P(VP-AMPS-$SiO_2$) has been successfully synthesized. The structure of the prepared hydrogel and composite were confirmed by FTIR, thermal analysis (TGA and DTA) and SEM micrograph. Batch adsorption studies for $La^{3+}$, $Ce^{3+}$, $Nd^{3+}$, $Eu^{3+}$ and $Pb^{+2}$ metal ions on the prepared hydrogel and composite were investigated as a function of shaking time, pH and metal ion concentration. The sorption efficiency of the prepared hydrogel and composite toward light rare earth elements (LREEs) are arranged in the order $La^{3+} > Ce^{3+} > Nd^{3+} > Eu^{3+}$. The obtained results demonstrated the superior adsorption capacity of the composite over the polymeric hydrogel. The maximum capacity of the polymeric composite was found to be 116, 103, 92, 76, 74 mg/gm for $La^{3+}$, $Ce^{3+}$, $Nd^{3+}$, $Eu^{3+}$ and $Pb^{2+}$ metal ions respectively.



## 1. Introduction

One of the commonly used methods for modifying the surface and bulk properties of polymeric materials is to template

* Corresponding author.

http://dx.doi.org/10.1016/j.jcis.2015.06.020
0021-9797/

monomers by irradiation technique known as radiation-induced template. Radiation-induced template method has the advantages such as simplicity, low cost, control over process and adjustment of the materials composition and structure. In addition, this method assures the template of monomers that are difficult to polymerize by conventional methods without residues of initiators and catalyst [1]. Radiation-induced template method is simply based on the irradiation of a base polymer either in the presence of a monomer (simultaneous radiation) or without a monomer (pre-irradiation) to create active sites.

In recent years, organic–inorganic polymer hybrids with a large variety of functionality have been studied intensively. The combination of the two components at a molecular level would provide novel properties that are hardly obtained from conventional organic or inorganic materials. There are different models to obtain silica composite. Contrary to the implementation of Stöber chemistry [2,3] or the microemulsion approach [4,5] the template method offers a very promising alternative route to circumvent the disadvantage of elevated temperatures, large amount of surfactants and/or organic solvents. In addition, the polymeric superstructures can also possess further chemical properties, e.g. for stimuli responsive release or entrapping of molecules.

Composite materials are used today in scientific, technological and manufacturing fields. Composite material is a product comprising a combination of dissimilar constituents. Many investigators have prepared composite sorbents, consisting of inorganic sorbents and organic binding matrices to overcome the limitations of organic resins and inorganic adsorbents [6,7]. Also different inorganic adsorbents such as clay minerals, zeolites, metal hydrates, metal phosphates, and metal oxides were handled in the preparation of composite sorbents.

Lanthanides represent an interesting group of elements which are steadily gaining importance in science and industry. They are now increasingly used in industry, medicine and agriculture. Therefore, the global needs for lanthanides will continue to grow during the next decades [8,9]. In this respect, the present work was oriented to prepare new hydrogel and composite sorbents by gamma radiation technique for effective adsorption of LREEs.

## 2. Experimental

### 2.1. Materials

Unless otherwise indicated, all materials were of analytical grade and were used without further purification. The lanthanide salts were obtained from Fluka Co. (Switzerland). Bi-distilled water was used for solvation, dissolution, dilution and analytical purposes. De-oxygenated water was used for preparation of hydrogel and composite.

### 2.2. Measurements

The samples were characterized by FTIR, Hartmann & Braun, Michelson, MB-Series 157 (Canada). Scanning electron microscope (SEM) photographs were recorded by JEOL-JSM 6510 LA (Japan) at accelerating voltage of 20 kV. A computerized UV/Vis double beam spectrophotometer of model T80, PG Instruments Ltd. (England), was used for spectrophotometric determination of metal ions. Thermal analysis was undertaken using a Shimadzu thermogravimetric analyzer model TGA-50 (Tokyo, Japan), a heating rate 10 °C/min, under nitrogen atmosphere (20 ml/min) from room temperature up to 800 °C. A cobalt-60 gamma cell of type MC-20 (Russia), was used as an irradiation source for polymerization at the Cyclotron Project, Inshas, Egypt.

### 2.3. Preparation of P(VP-AMPS) hydrogel

P(VP-AMPS) resin was prepared by template polymerization of 2-Acrylamido 2-methyl propane sulphonic acid monomer onto poly(vinyl pyrilidone) P(VP) as a template polymer in the presence of N,N′-methylenediacrylamide (DAM) as a crosslinker.

About 0.5 g of PVP dissolved in 50 ml bi-distilled water and mixed with 0.6 g of DAM. 10 g of AMPS were dissolved in another 50 ml bi-distilled. The two solutions were mixed using mechanical stirrer for 20 s then transferred into glass ampoules. Nitrogen gas was purged into the ampoules to remove the air from the solutions. The glass ampoules were sealed and then subjected to gamma-irradiation at dose 20 kGy at ambient temperature. After irradiation process, the resin was cut into small discs with a stainless steel scissors. The entire prepared resin was immersed twice in excess bi-distilled water and acetone for 4 h to remove the un-reacted monomers. The prepared resin was treated with 0.1 N NaOH to convert the resin into sodium form then left to dry at room temperature.

### 2.4. Preparation of P(PVP-AMPS-$SiO_2$) composite

Poly(PolyAcrylamide-sodium styrene sulphonate-silicon oxide) P(AM-AMPS-$SiO_2$) composite was prepared by radiation induced polymerization of Polyacrylamide polymer with sodium styrene sulphonate monomers and silicon oxide in de-oxygenated water in the presence of DAM as a crosslinking agent.

About 0.5 g of PVP dissolved in 50 ml bi-distilled water and 0.6 g of DAM, 10 g of AMPS. 0.6 gm of silica was dissolved in 50 ml bi-distilled water. The two solutions were mixed then transferred into glass ampoules and nitrogen gas was purged into the ampoules to remove air from the solutions. The glass ampoules were sealed and then subjected to gamma-irradiation at dose 20 kGy in air at ambient temperature. After irradiation process, the composite was cut into small discs. The entire prepared composite was immersed twice in excess bi-distilled water and acetone for 4 h to remove the un-reacted monomers.

### 2.5. Sorption studies

The batch experiments of the prepared polymeric hydrogel and composite for the adsorption of $La^{3+}$, $Ce^{3+}$, $Nd^{3+}$, $Eu^{3+}$ and $pb^{2+}$ metal ions from aqueous solution were carried out using a thermostatic water bath shaker at 25 °C for 24 h. Dried samples of each of resin and composite 0.05 gm were stirred in a 10 mL of the aqueous solution. The concentration of the metal ions in solution was determined by computerized UV/Vis double beam spectrophotometer using 4-(Pyridyl-2-azo) resorcinol (PAR) as sensitive coloring reagent. Based on the initial and final metal concentrations, the amount adsorbed (mg/g) and percent uptakes were calculated as follows:

$$q(\mathrm{mg/g}) = \frac{(C_i - C_e)V}{m} \quad (1)$$

$$\%\mathrm{uptake} = \frac{(C_i - C_e)}{C_i} 100 \quad (2)$$

where ($q$) is the maximum capacity (mg/gm), $C_i$ and $C_e$ are the initial and equilibrium concentrations (mg/L) of metal ions respectively. $V$ is the volume of solution in liter and $m$ is the weight of the resin in gm.

The effect of shaking time was investigated at different period from 5 min to 24 h, at 30 °C, pH = 4 and metal ion concentration 100 mg/L. The effect of pH was tested at different values ranging from 1.0 to 5.0. The initial metal concentration was carried out at various initial metal concentration ranged from 100 to

2000 mg/L. After shaking the mixture was centrifuged and filtrated using 0.45 μm Whatman membrane filter and the amount of metal ion remaining in the filtrate was measured by using A computerized UV/Vis double beam spectrophotometer.

### 2.6. Mathematical calculations to investigate the degree of polymerization

Series of experiments were carried out to test the effect of monomer, polymer, crosslinker concentrations and the irradiation dose on the swelling degree, percent conversion and resin capacity. The resin capacity was evaluated by mixing 10 ml of $Cu^{2+}$ solution with 0.01 gm of studied resin that was already prepared in sodium form. The mixture was centrifuged and filtrated [10]. The concentration of $Cu^{2+}$ metal ions was measured and the capacity was calculated according to Eq. (1).

Swelling degree of the resin was evaluated to explain the physico-chemical behavior of polymer in water. In this respects, 50 mg of resin was kept in 10 ml of aqueous solution for 24 h at room temperature. After filtration, the surface water on the swollen resin sample was removed by softly pressing between the folds of filter paper. An increase in resin weight was measured and the swelling degree ($P_S$) was calculated according to Eq. (3) as following:

$$P_S = \frac{(Wf - Wi)}{Wi} 100 \quad (3)$$

where *Wf* is the weight of the swollen polymer and *Wi* is the weight of dry polymer.

Percent conversion of the reactants into polymeric resin was calculated at different reaction parameters such as monomer, polymer, crosslinker concentrations and irradiation dose. This percentage was used as indicator to get the maximum conversion yield and it was calculated as shown in Eq. (4)

$$\%\text{conversion} = \frac{(W)}{Ws} 100 \quad (4)$$

where *W* is the weight of polymer and *Ws* is the weight of add reactants.

## 3. Results and discussion

### 3.1. Preparation of P(VP-AMPS) hydrogel

The polymerization process is strongly influenced by synthesis conditions such as monomer, polymer and crosslinker concentrations and irradiation dose. Therefore, the effects of these reaction parameters were investigated. The presence of water produces after irradiation especially hydroxyl free radicals are very effective in the degree of polymerization. Various possible interaction are expected including the hydrogen bonding formed between P(AMPS) and P(VP), strong intermolecular affinity between the polymer chains and the hydrogen bonding between the sulphonic groups of P(AMPS) and carbonyl groups of P(VP). These interactions are mainly responsible for the interpolymer association as described in Scheme 1.

#### 3.1.1. Effect of AMPS weight on the polymerization process

The effect of AMPS monomer concentration on the polymerization yield was tested at 2.0–14 wt%. The polymerization process was performed at irradiation dose of 10.0 kGy, P(VP) concentration of 0.5 wt% and 0.3 wt% of the crosslinker. The capacity of the obtained hydrogel toward $Cu^{2+}$, the conversion percent and swelling degree were demonstrated in Fig. 1a –c respectively.

Fig. 1a shows that the capacity increases with increasing the monomer concentration till 10 wt% and then decreases. The maximum metal ion capacity was achieved at 10 wt% of AMPS. This behavior suggests that the diffusivity of monomer into the polymer matrix is enhanced at high concentrations and the number of sulphonic groups increases resulting in higher capacity. Fig. 1b shows that the swelling degree increases with increasing monomer concentration till concentration 12 wt% and then decrease. On increasing the monomer concentration, the probability of the association between the monomer and the added polymer increases which, increases the degree of crosslinking (permanent trapped entanglements) between the polymer chains of the resin. After 12 wt%, the polymer refuses to accept anymore of the solvent and the swelling degree decreases. Fig. 1c shows that the percent conversion increases with increasing monomer concentration. This may be due to increase the crosslinking between the monomer and added polymer of the resin.

#### 3.1.2. Effect of P(VP) on the polymerization process

The effect of polymer concentration ranging from 0.1 to 2.0 wt% on the polymerization yield was tested and the data presented in Fig. 2a–c.

Fig. 2a shows that the capacity of the resins toward $Cu^{2+}$ increases till 0.5 wt% and then decreases with increasing the polymer concentration. The maximum capacity was achieved at 0.5 wt% PVP. On increasing the amount of added polymer, increases the crosslinking association between the monomer and the added polymer which, increase the capacity. After 0.5 wt% the crosslinking between the polymer chains increases to the extent at which, the metal ion will be rejected hence, the capacity of the resin decreases. Fig. 2b shows that the swelling degree increases with increasing the PVP concentration till 0.5 wt% then decreases with further increases of PVP concentration. After 0.5 wt%, the polymer matrix becomes satisfy by solvent molecules around the chains between the network junctions. Consequently, the swelling degree of the resin decreases. Fig. 2c shows that the percent conversion increases with increasing of PVP concentration, which can be attributed to increase of the crosslinking and probability of association between the monomer and polymer chains of the resin.

#### 3.1.3. Effect of irradiation dose on the polymerization process

The effect of adsorbent dose on polymerization process was investigated at PVP concentration 0.5 wt%, AMPS concentration of 10 wt%, 0.3 wt% DAM as crosslinker and various irradiation doses ranged from 2.0 to 30.0 kGy. The results are presented in Fig. 3a–c. Fig. 3a shows that the capacity increases till the irradiation dose reach to 20 kGy and then rapidly decreases with increasing of irradiation dose. The decrease in the capacity can be attributed to the higher increase in the extent of crosslinking which, decrease in the number of active function groups. The maximum capacity was achieved at irradiation dose 20.0 kGy. Fig. 3b shows that swelling degree decrease with the increasing of irradiation dose, which can be attributed to the decrease in the crosslinking between the polymeric chains of the resin and the diffusion processes from the solution to the resin. Fig. 3c shows that the percent conversion increases till irradiation dose 25 kGy and constancy state occurs with no apparent further increase. This may be due to increase the crosslinking and probability of association between the polymer matrixes.

#### 3.1.4. Effect of DAM concentration on the polymerization process

Fig. 4 shows the effect of crosslinker concentration on the polymerization yield at polymer concentration 0.5 wt%, AMPS concentration of 10 wt%, irradiation dose 20.0 kGy and different DAM concentration ranging from 0.1 to 1.0 wt%.

Fig. 4a shows that the capacity of the polymer increase till 0.6 wt% and then decreases with increasing of DAM concentration.

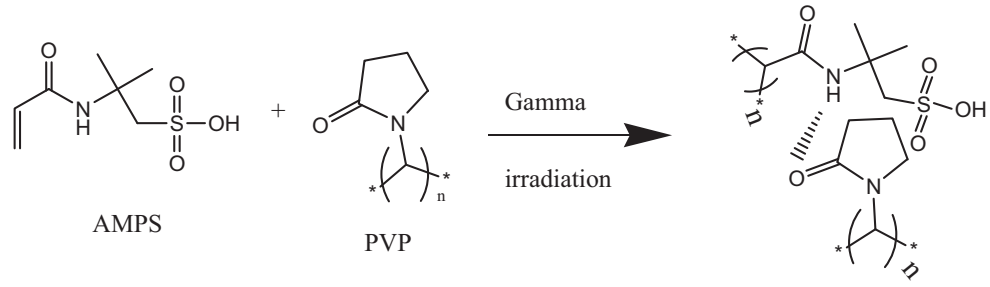


**Scheme 1.** The expected structure of P(VP-AMPS) hydrogel.

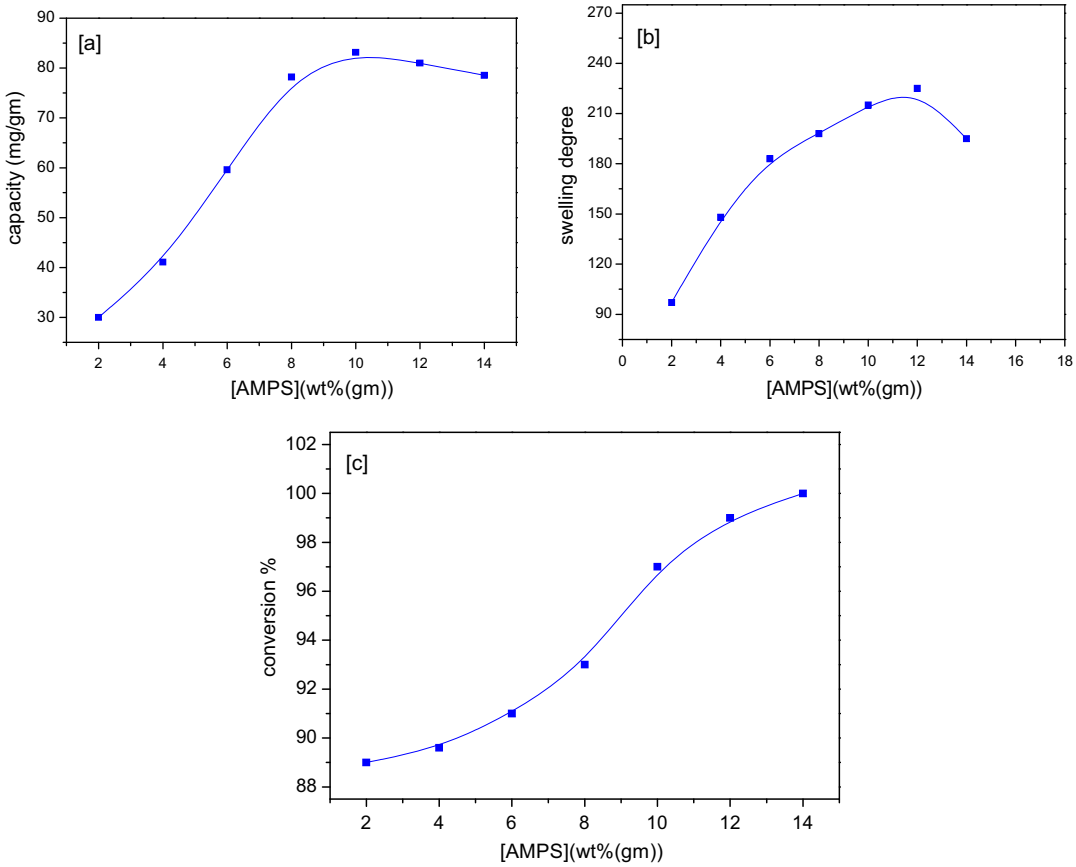


**Fig. 1.** Influence of the monomer concentration on (a) capacity, (b) swelling degree and (c) conversion yield of P(VP-AMPS) hydrogel.

i.e. The maximum $Cu^{2+}$ metal ion capacity was achieved at 0.6 wt% at which, the attachment between the polymer and monomer in the network junctions be proportionate and saturated without deterioration of the available function groups. Fig. 4b shows that the swelling degree decreases with increasing the concentration of crosslinking agent. With the higher increasing in the extent of crosslinker, the chain reaction between network junctions of the resin decreases which, decrease the swelling degree. Fig. 4c shows that the conversion percentage increases with the increasing of crosslinker and reached to steady state in the range from 0.6 to 1.0 wt%.

Through the previous result, it was found that the optimum conditions for preparation of P(VP-AMPS) hydrogel could be obtained at polymer concentration 0.5 wt%, AMPS concentration 10 wt%, irradiation dose 20.0 kGy and DAM concentration of 0.6 wt%. At these conditions, the percent conversion was found to be 100% while, the swelling degree reached to 146 and the maximum capacity toward $Cu^{+2}$ metal's ion was 91 mg/gm. Fig. 5 showed the physical appearance of the prepared hydrogel which characterized by high swelling degree.

### 3.2. Preparation of P(PVP-AMPS-$SiO_2$) Composite

Polymerization of (AMPS) on P(VP) as a template polymer was takes place by gamma-radiation induced template polymerization in the presence of DAM as a cross-linker and silicone oxide that was extracted from rice husk ash. The expected structure of the composite is presented in Scheme 2.

The influence of silica concentration on the capacity toward $Cu^{2+}$, percent conversion and the swelling degree of the obtained composite was studied at a polymer concentration 0.5 wt%, AMPS concentration of 10 wt%, irradiation dose 20.0 kGy, DAM concentration of

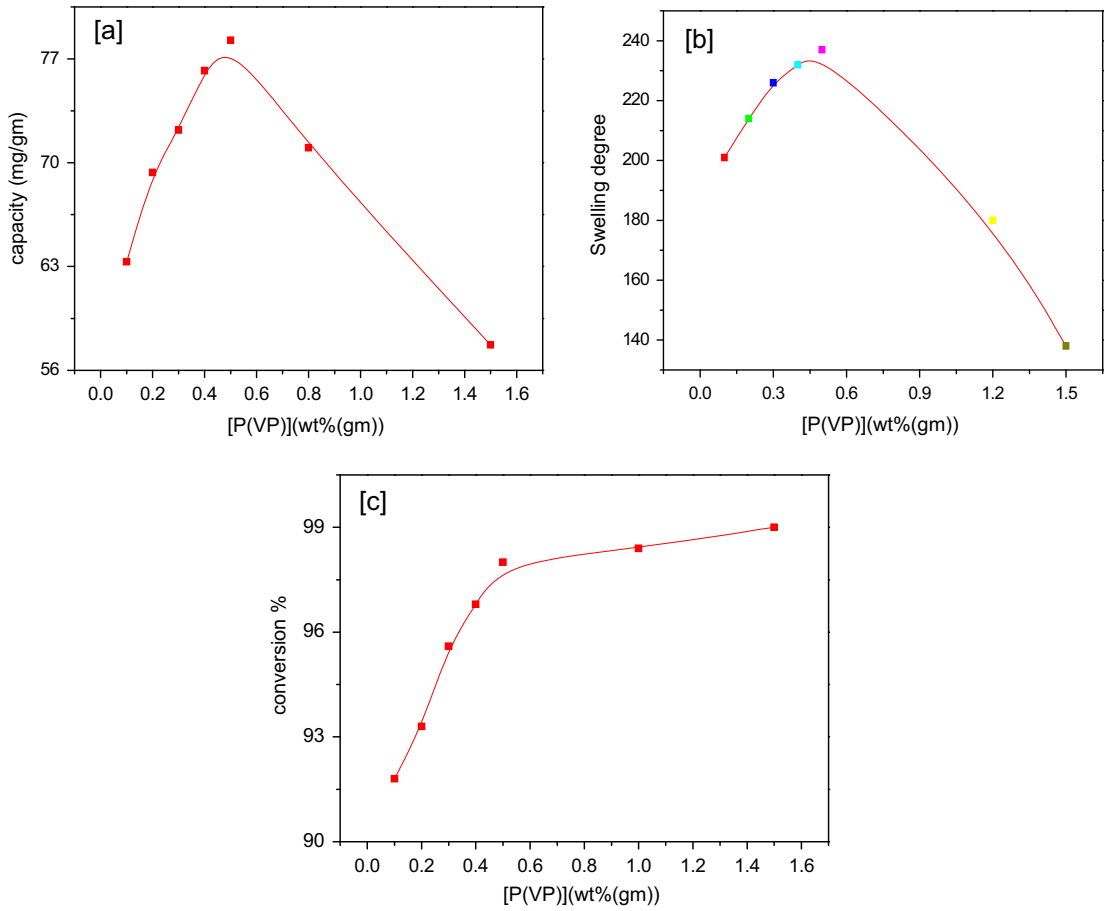


**Fig. 2.** Influence of P(VP) concentration on (a) capacity, (b) swelling degree and (c) conversion yield of P(VP-AMPS) hydrogel.

0.6 wt% and different silicon oxide concentration ranged from 0.1 to 0.7 wt%. The obtained results are shown in Fig. 6a–c.

The optimum condition for preparation of P(VP-AMPS-$SiO_2$) composite was found at polymer concentration 0.5 wt%, AMPS concentration of 10 wt%, irradiation dose 20.0 kGy, DAM concentration of 0.6 wt% and silicon oxide concentration of 0.3 wt%. Due to the presence of silica, the prepared composite have a significantly higher sorption capacity toward Cu(II) reached to 99.8 mg/g. Swelling degree found to be 341 and percent conversion was reduced to 92%. Fig. 7 showed the physical appearance of the prepared composite which characterized by high swelling degree.

### 3.3. Characterization of the prepared polymeric hydrogel and composite

#### 3.3.1. FTIR analysis

As shown in Fig. 8a, FTIR spectrum indicates that, hydrogen bonding is forming between P(AMPS) network and linear P(VP). The stretching frequency of >C═O give absorption peak at 1650 $cm^{-1}$. The free >NH stretching give absorption peak at 3334 $cm^{-1}$ [10]. The absorption peak at 1042 $cm^{-1}$ indicates the presence of C—H monosubstituted $SP^2$ bending [11]. The absorption peak at 2810 $cm^{-1}$ indicates the presence of C—H monosubstituted $SP^3$ stretching [12]. The absorption peaks appeared at 1550, 3334 and 1654 $cm^{-1}$ are attributed to contributions of carbonyl (—C═O), amide NH stretching and amide NH bending groups of AMPS and PVP, respectively [10]. The absorption peaks at 1038 $cm^{-1}$ and 1201.6 $cm^{-1}$ represent symmetric and asymmetric stretching in O═S═O [13]. The peak at 622.5 $cm^{-1}$ confirms the presence of —S—O stretching bond [14]. The presence of these peaks verifies the polymerization of PVP with AMPS by gamma-radiation technique.

FTIR spectrum of the polymeric silica composite is shown in Fig. 8b. The spectrum indicates that hydrogen bonding is forming between P(AMPS) network and linear P(VP). The stretching frequency of >C═O give absorption peak at 1561 $cm^{-1}$, free >NH stretching and bending give absorption peak at 3444 and 1621 $cm^{-1}$ [14]. Water shows an intense characteristic absorption band at 3067 $cm^{-1}$ assigned to O—H stretching in H-bonded water. The latter band can be cross checked through the 1635 $cm^{-1}$ band due to scissor bending vibration of molecular water. In addition, the following bands observed, stretching C—H band ($CH_2$ groups) at 2978 $cm^{-1}$ and bending C—H $sp^3$ band at 1396 $cm^{-1}$. The absorption peaks at 1038 $cm^{-1}$ and 1201.6 $cm^{-1}$ represent symmetric and asymmetric stretching in O═S═O [13]. The peak at 622.5 $cm^{-1}$ confirms the presence of —S—O stretching bond [15]. Absorption bands arising from asymmetric vibration of Si—O (1090 $cm^{-1}$) and symmetric vibration of Si—O (795 $cm^{-1}$). The absorption bands between 800 and 1260 $cm^{-1}$ have been described as a superimposition of various $SiO_2$ peaks. Therefore, it could be concluded that the polymerization of P(VP-AMPS-$SiO_2$) composite is successfully confirmed.

#### 3.3.2. SEM analysis

The compositions of the prepared hydrogel and composite show clearly a significant difference in the topography of the surface. SEM morphology of the P(VP-AMPS) hydrogel exhibits rough surface pattern and many pores appear. They are usually curved and

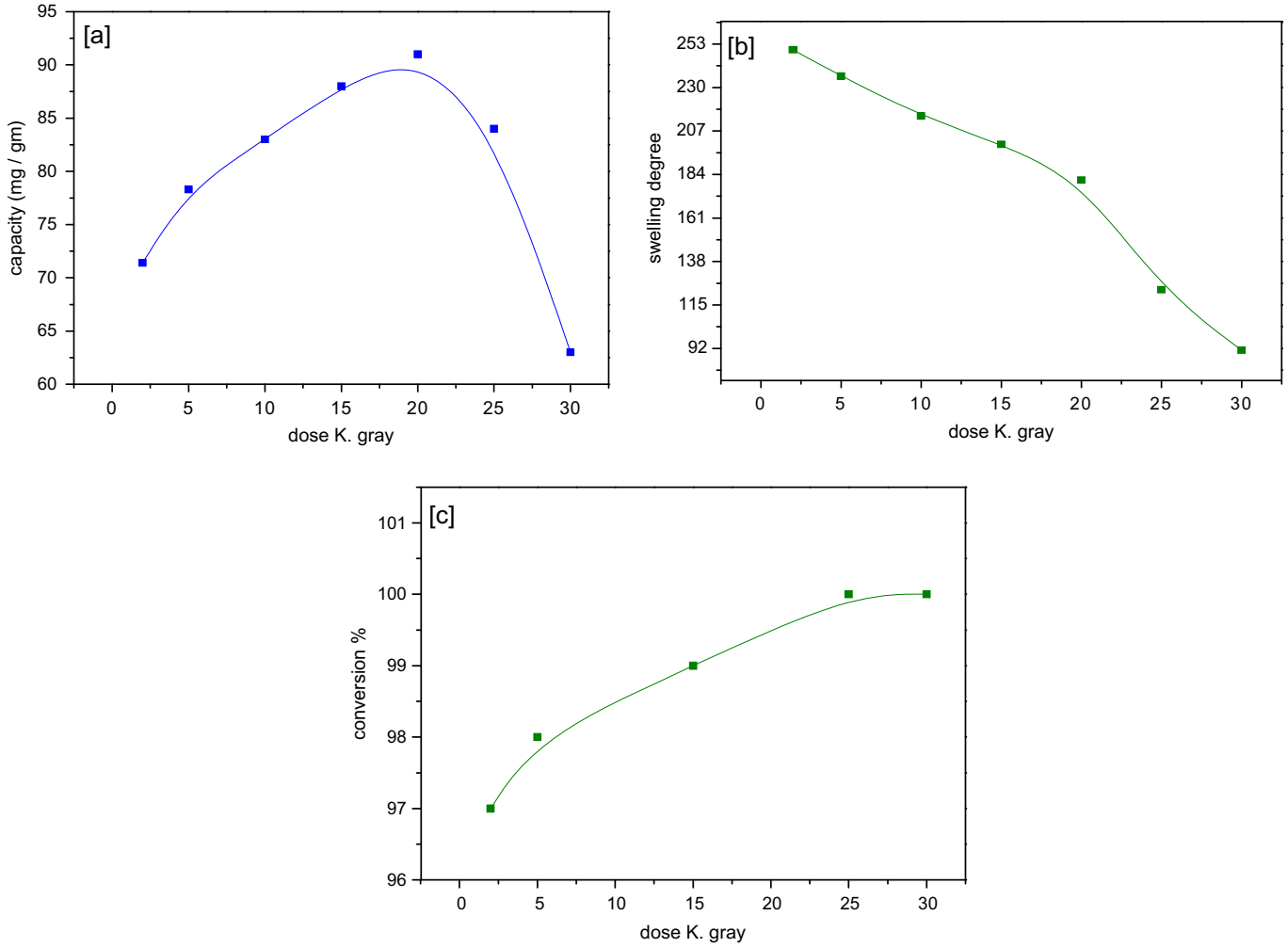


**Fig. 3.** Influence of the irradiation dose on (a) capacity, (b) swelling degree and (c) conversion yield of P(VP-AMPS) hydrogel.

entangled with each other. Moreover, the polymer appeared to be piled up with thick scales. The AMPS monomers were uniformly distributed into P(AMPS) which, increasing the surface area of the polymeric hydrogel as shown in Fig. 9a. The SEM morphology of P(VP-AMPS-$SiO_2$) composite, exhibits a very rough surface and lots of raised or etched strips and stops. The reason for the surface roughness is due to the presence of silica. Furthermore, the gamma irradiation of AMPS and PVP opens up its matrix and create holes on the surface of back bone of the composite as shown in Fig. 9b. So the rough surface structure with many pores may be reflecting the high capacity of the produced polymer/silica composite comparing with the polymer hydrogel without silica [16].

### 3.3.3. TGA analysis

TGA (DTA) thermograms of P(VP-AMPS) illustrated in Fig. 10a, indicating the presence of four peaks relating to three thermal decomposition steps of the macromolecules fragments [17]. The degradation of P(VP-AMPS) hydrogel proceeds in three stages. The first stage from 50 to 200 °C with a maximum endothermic peak at 94.37 °C exhibits a weight loss of 20.380% which, may be due to the removal of absorbed or coordinated water molecules. The second stage from (200 to 407) °C shows endothermic peaks at 207–332 °C with a weight loss of 53.2% which, may be attributed to desulphonation of sulphonic acid and release of $SiO_2$. The third stage at 407–1000 °C shows endothermic peak at 747.93 °C with the weight loss of 27.96% which, may be due to removal of volatile hydrocarbons and complete degradation to the oxide form. The same condition for analysis carried out P(VP-AMPS-$SiO_2$) composite shown in Fig. 10b. The thermal degradation occurs via three stages. The first stage from 50 to 184 °C may be attributed to removal of all surface and matrix-bound moisture from the polymeric composite [96], with the weight loss of 8.864%. The second stage from 184 to 527 °C which can be attributed to desulphonation of sulphonic acid with the weight loss of 64.9%. The third stage from 527 to 1000 °C may be due to chain scission, removal of volatile hydrocarbons, complete degradation to the oxides and the possibility of metal carbide formation [17].

The TGA and DTA charts of dried P(VP-AMPS-$SiO_2$) composite sample heated at the rate of 10 °C/min are shown in Fig. 10b. The thermal degradation occurs via three stages. The first stage from 50 to 184 °C may be attributed to removal of all surface and matrix-bound moisture from the polymeric composite [18], with the weight loss of 8.864%. The second stage from 184 to 527 °C is attributed to desulphonation of sulphonic acid with the weight loss of 64.9%. The third stage from 527 to 1000 °C may be due to chain scission, removal of volatile hydrocarbons, complete degradation to the oxides and the possibility of metal carbide formation [19].

## 3.4. Sorption behavior of metal ions

### 3.4.1. Metal hydrolysis

Series of experiments have been tested separately to evaluate the degree of contribution of the two reaction mechanisms (sorption and precipitation) at different pH range to avoid the metal

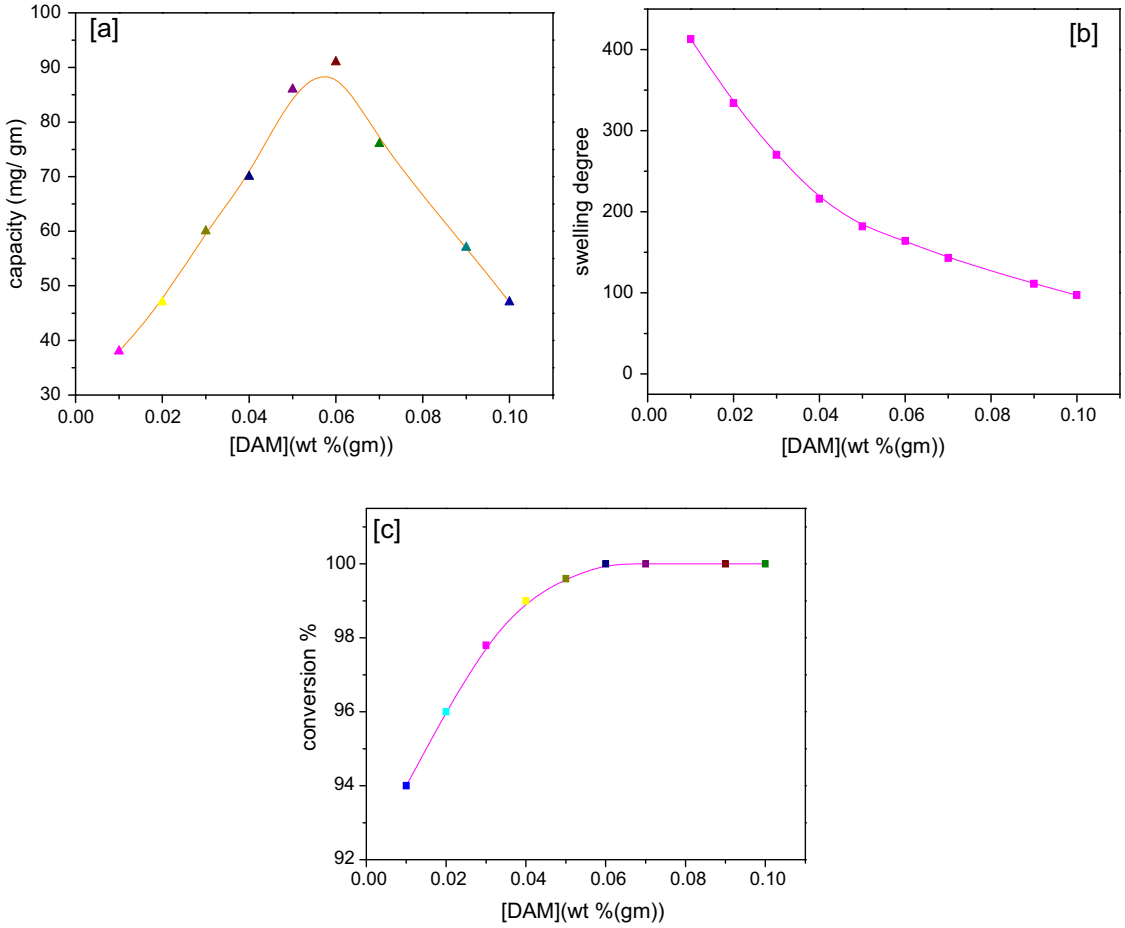


**Fig. 4.** The effect of DAM concentration on (a) capacity, (b) swelling degree and (c) conversion yield of P(VP-AMPS) hydrogel.

**Fig. 5.** Physical appearance of P(VP-AMPS) hydrogel.

ion hydrolysis of $La^{3+}$, $Ce^{3+}$, $Nd^{3+}$, $Eu^{3+}$ and $Pb^{2+}$ metal's ion. The experiments were carried out at 100 mg/L of each metal's ion at different pH values. The data (not presented for brevity) showed that partial hydrolysis was observed at pH = 6 for all the investigated metal ions. Therefore, all the upcoming sorption experiments were carried at in the pH range from 1 to 5.

*3.4.2. Sorption of LREEs and $pb^{2+}$ ions on P(VP-AMPS) hydrogel and P(VP-AMPS-$SiO_2$) composite*

*3.4.2.1. Effect of contact time.* The extent of contact time interaction between $La^{3+}$, $Ce^{3+}$, $Nd^{3+}$, $Eu^{3+}$, $pb^{2+}$ metal ions with the polymer and composite were studied by batch equilibration technique at initial concentration 100 mg/L and 0.05 gm of modified polymeric hydrogel and composites.

The results presented in Fig. 11a–e, shows the sorption behavior of the investigated metal ions on P(PVP-AMPS) hydrogel in both H and Na forms and P(VP-AMPS-$SiO_2$) composite. The results indicate that the rate of metal-ion uptake increases rapidly till reaches to steady state at 3 h for the three investigated sorbents. This finding could be explained firstly, the fact that, the adsorption sites are highly available and the metal ions can interact easily with the existing pores on the surface, so high adsorption rate is obtained. Besides, the driving force for adsorption is the concentration gradient between the bulk solution and the solid–liquid interface. This concentration gradient is high in the initial period, which results in a high adsorption rate. A slow adsorption at the inner surface was then observed because of pore diffusion of metal solution into the component matrix.

The maximum uptake for modified polymeric resins and composite were found to be (53, 67, 84) for ($La^{3+}$), (49, 64, 81) for $Ce^{3+}$, (44, 61, 78) for $Nd^{3+}$, (37, 46, 54) for $Eu^{3+}$, (32, 40, 44) for $Pb^{2+}$ on P(PVP-AMPS) hydrogel in H and Na form and P(VP-AMPS-$SiO_2$) composite respectively. The results demonstrated that the metal uptake of the composite is higher than the corresponding values of the hydrogel in both H and Na forms. This may be due to the presence of silica which provides larger voids, possible channels and cavities that may be facilitate the movement of the metal ions, besides the presence of effective function groups.

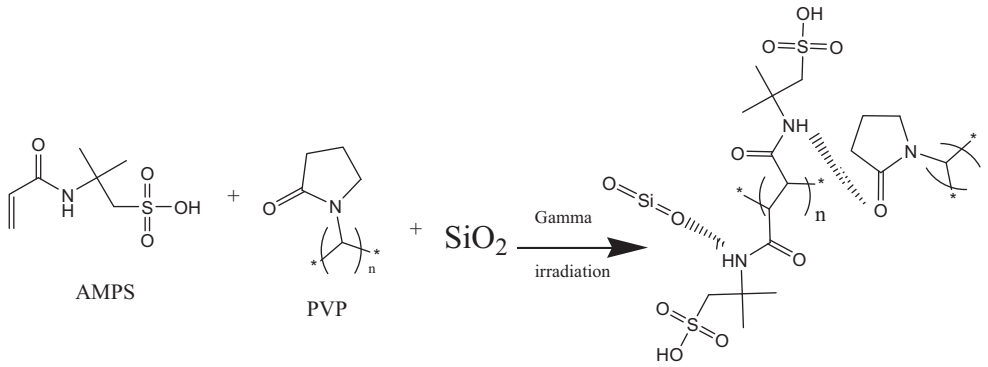


**Scheme 2.** Synthesis and the expected structure of P(VP-AMPS-$SiO_2$) composite.

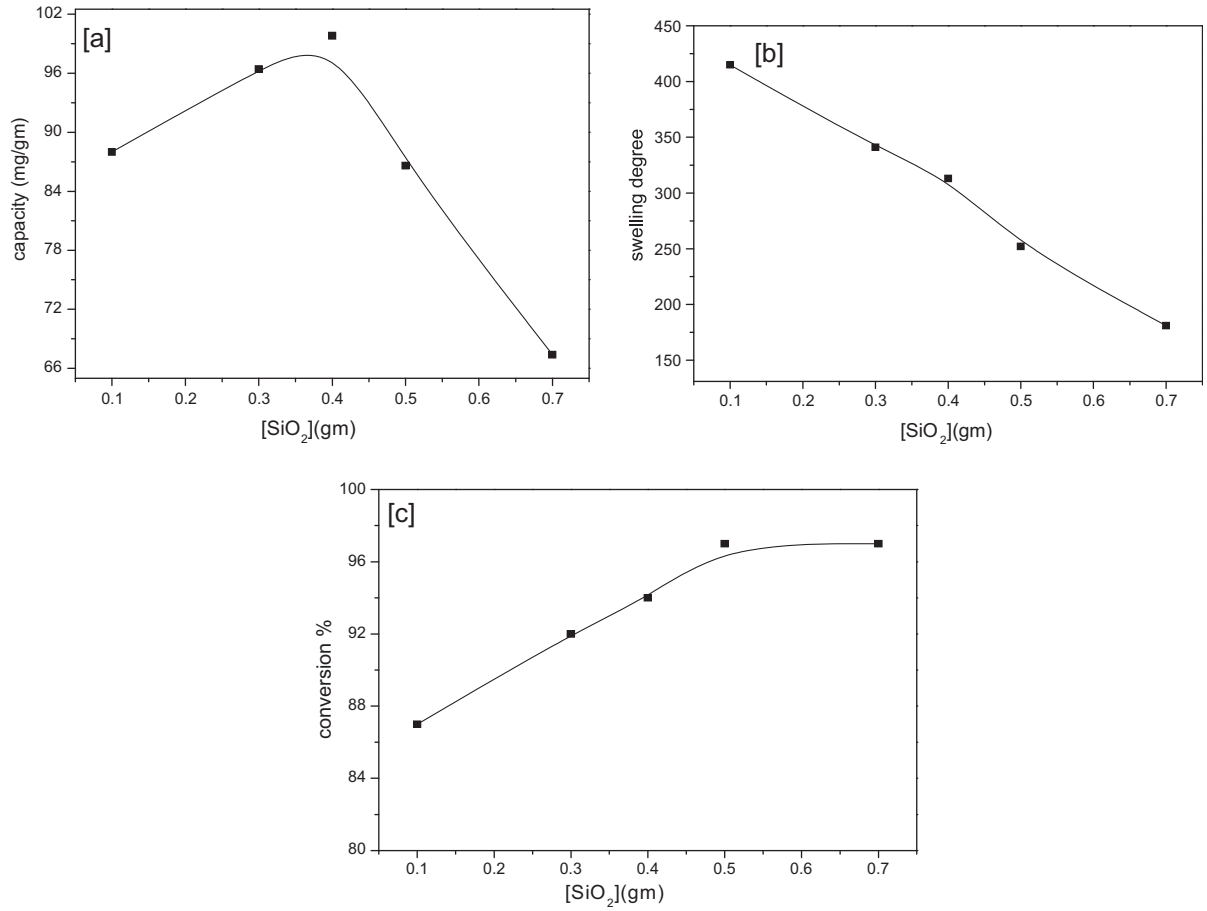


**Fig. 6.** Influence of the $SiO_2$ concentration on (a) capacity, (b) swelling degree and (c) conversion yield P(VP-AMPS-$SiO_2$) composite.

Metal-ion uptake observed for these polymeric hydrogel and composite follows the order $La^{3+} > Ce^{3+} > Nd^{3+} > Eu^{3+} > Pb^{2+}$. The sorption behavior is in a good agreement electro positivity of lanthanides which, decreases from La to Eu metal ions.

Note that the hydrated radii of tri positive elements are increasing as proceed from La to Eu [20], thereby confirming the fact that there is a contraction in the size of these molecules, so the smaller ionic size of La ions helps in its easy approach to less approachable sites of the adsorbent as compared to that of Eu ions and found that P(VP-AMPS-$SiO_2$) composite displayed the highest metal-ion uptake toward metal's ion over than P(PVP-AMPS) in (Na form) and P(PVP-AMPS) in (H form), respectively.

*3.4.2.2. Effect of pH.* The role of hydrogen ion concentration on the uptake of $La^{3+}$, $Ce^{3+}$, $Nd^{3+}$, $Eu^{3+}$, $Pb^{+2}$ on P(VP-AMPS) hydrogel and P(VP-AMPS-$SiO_2$) composite was examined in the pH range 1–5 at fixed contact time of 6 h.

As shown in Fig. 12, the percent adsorption for $La^{3+}$, $Ce^{3+}$, $Nd^{3+}$, $Eu^{3+}$, $Pb^{+2}$ metal ions increased with increasing pH and reached the plateau at pH 5 for all the metal ions. The maximum adsorption took place at pH 5.0. It is clear that, P(VP-AMPS-$SiO_2$) composite is more effective for the quantitative removal of $La^{3+}$, $Ce^{3+}$, $Nd^{3+}$, $Eu^{3+}$ and $Pb^{+2}$ metal ions than P(VP-AMPS) hydrogel in both H and Na form, respectively. Furthermore, the maximum uptakes for metal ions are arranged in the following order:

**Fig. 7.** Physical appearance of P(VP-AMPS-$SiO_2$) composite.

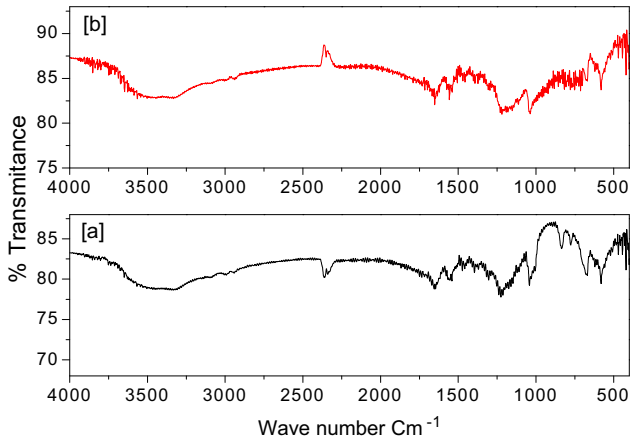


**Fig. 8.** FTIR spectrum of (a) P(VP-AMPS) hydrogel and (b) P(VP-AMPS-$SiO_2$) composite.

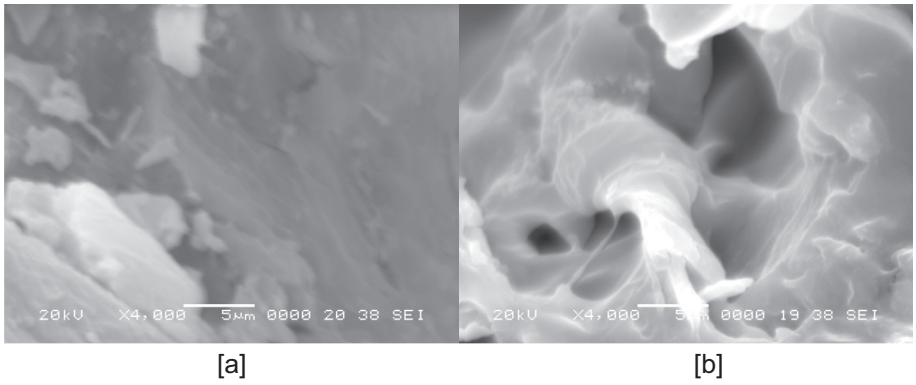


**Fig. 9.** SEM of (a) P(VP-AMPS) hydrogel and (b) P(VP-AMPS-$SiO_2$) composite.

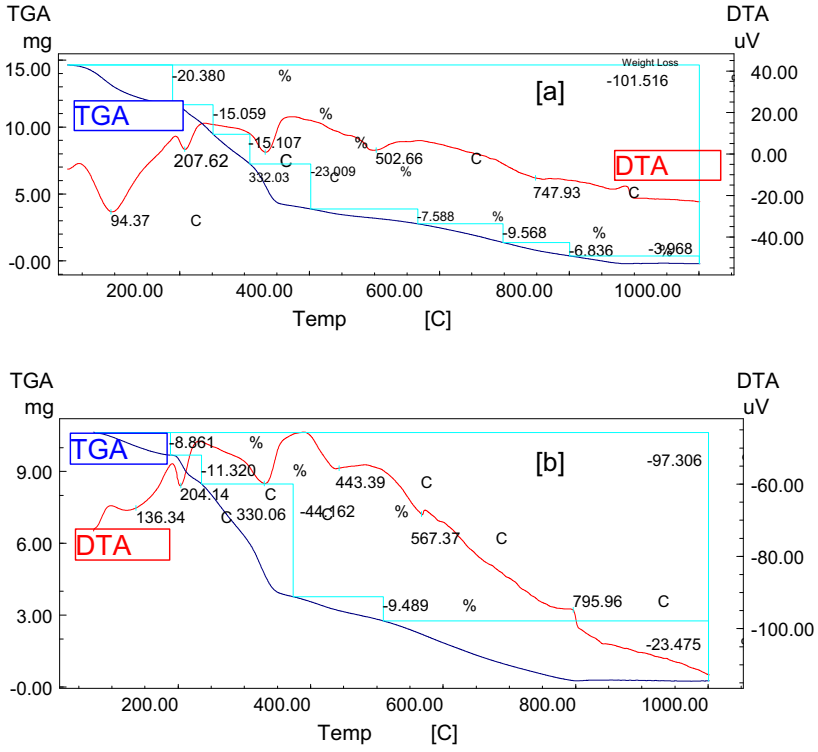


**Fig. 10.** TGA and DTA curves for (a) P(VP-AMPS) hydrogel, (b) P(VP-AMPS-$SiO_2$) composite.

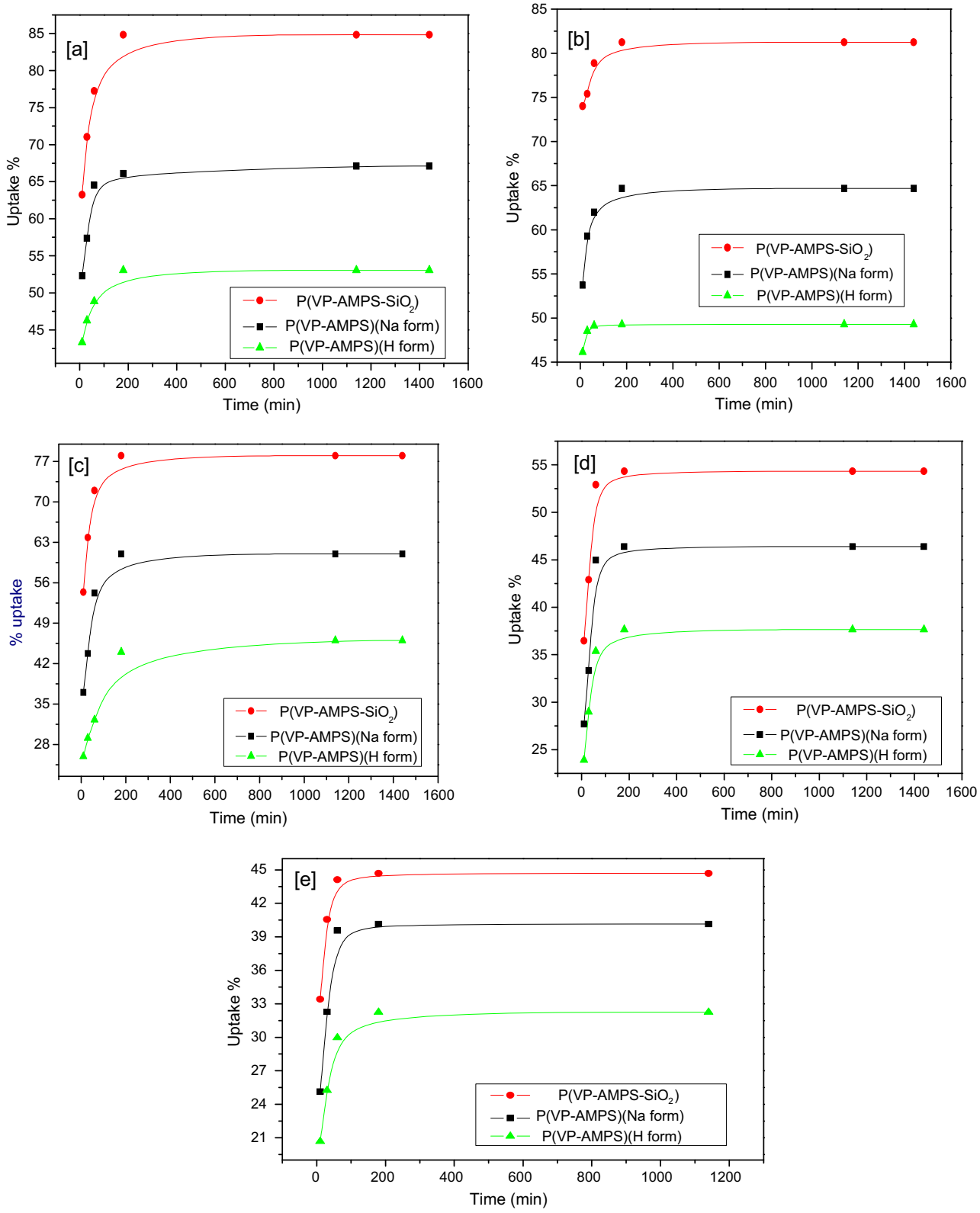


**Fig. 11.** The effect of time on metal ions uptake of (a) $La^{3+}$, (b) $Ce^{3+}$, (c) $Nd^{3+}$, (d) $Eu^{3+}$ and (e) $pb^{2+}$ on P(VP-AMPS) hydrogel in (H and Na form) and P(VP-AMPS-$SiO_2$) composite.

$La^{3+} > Ce^{3+} > Nd^{3+} > Eu^{3+} > Pb^{2+}$

The adsorption behavior of the metal ions on P(VP-AMPS-$SiO_2$) and P(VP-SSS) hydrogel (H and Na form) occurred probably by ion exchange mechanism. This mechanism is evidently suggested because P(VP-AMPS) is basically contains PVP and AMPS. The polar functional groups of P(VP-AMPS) e.g., sulphonic group is involved in these processes. It is affected by pH and may undergo deprotonation thereby resulting in the variation in surface charge of the adsorbent [20,21]. At higher acidic conditions, i.e., low pH value

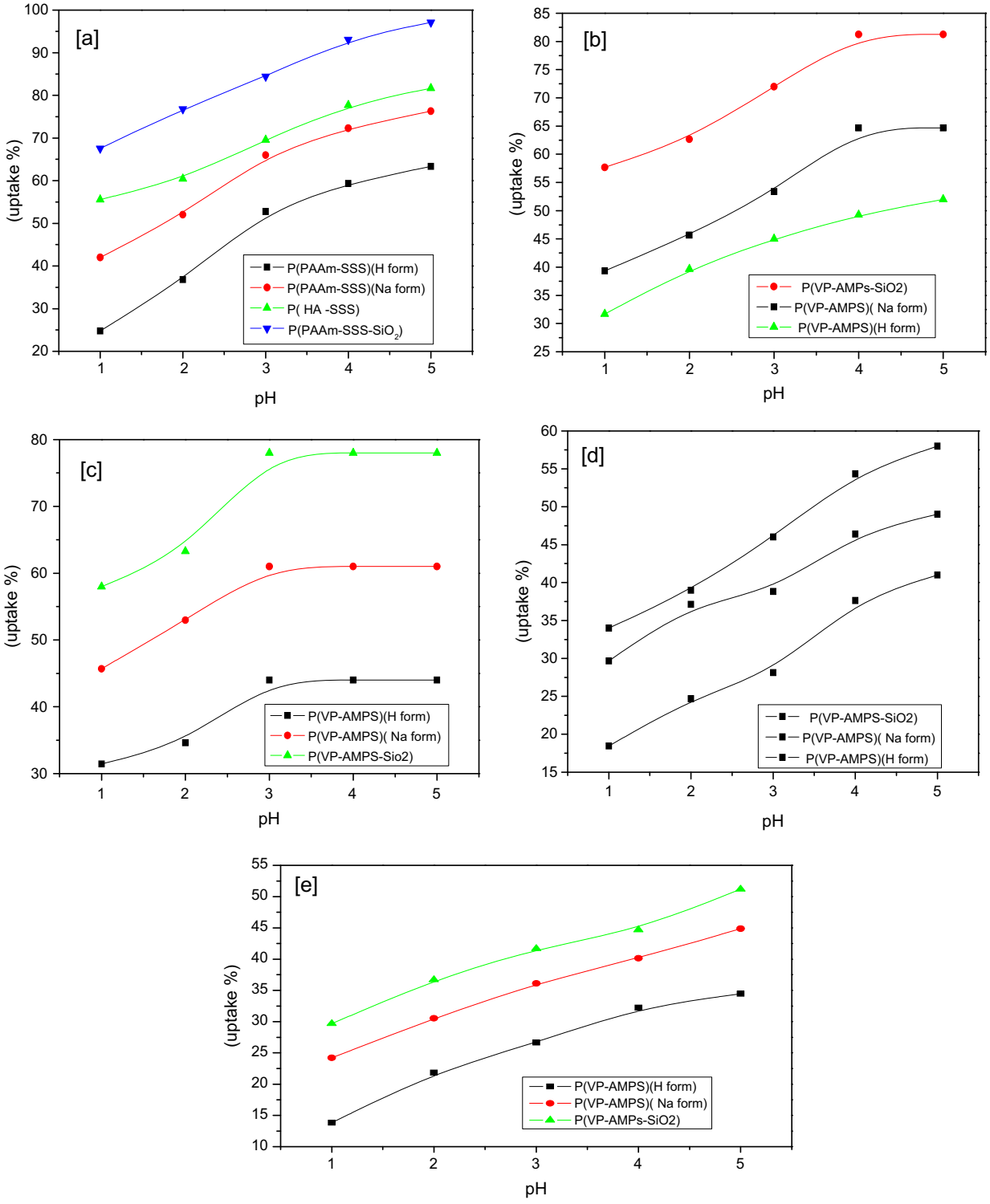


**Fig. 12.** The effect of pH on the sorption percent of (a) $La^{3+}$, (b) $Ce^{3+}$, (c) $Nd^{3+}$, (d) $Eu^{3+}$ and (e) $pb^{2+}$ metal ions on P(VP-AMPS) hydrogel in (H and Na form) and P(VP-AMPS-$SiO_2$) composite.

of about 1.0–2.0, low adsorption of metal ions was occurred. This is attributed to the competition between H + ions and metal's ions for the active function groups (sulphonic groups) on the adsorbent surface. With the increase of the pH of the solution, deprotonation process increases, the amount of adsorbed metal ions increases and maximum adsorption was obtained at pH of 5.0.

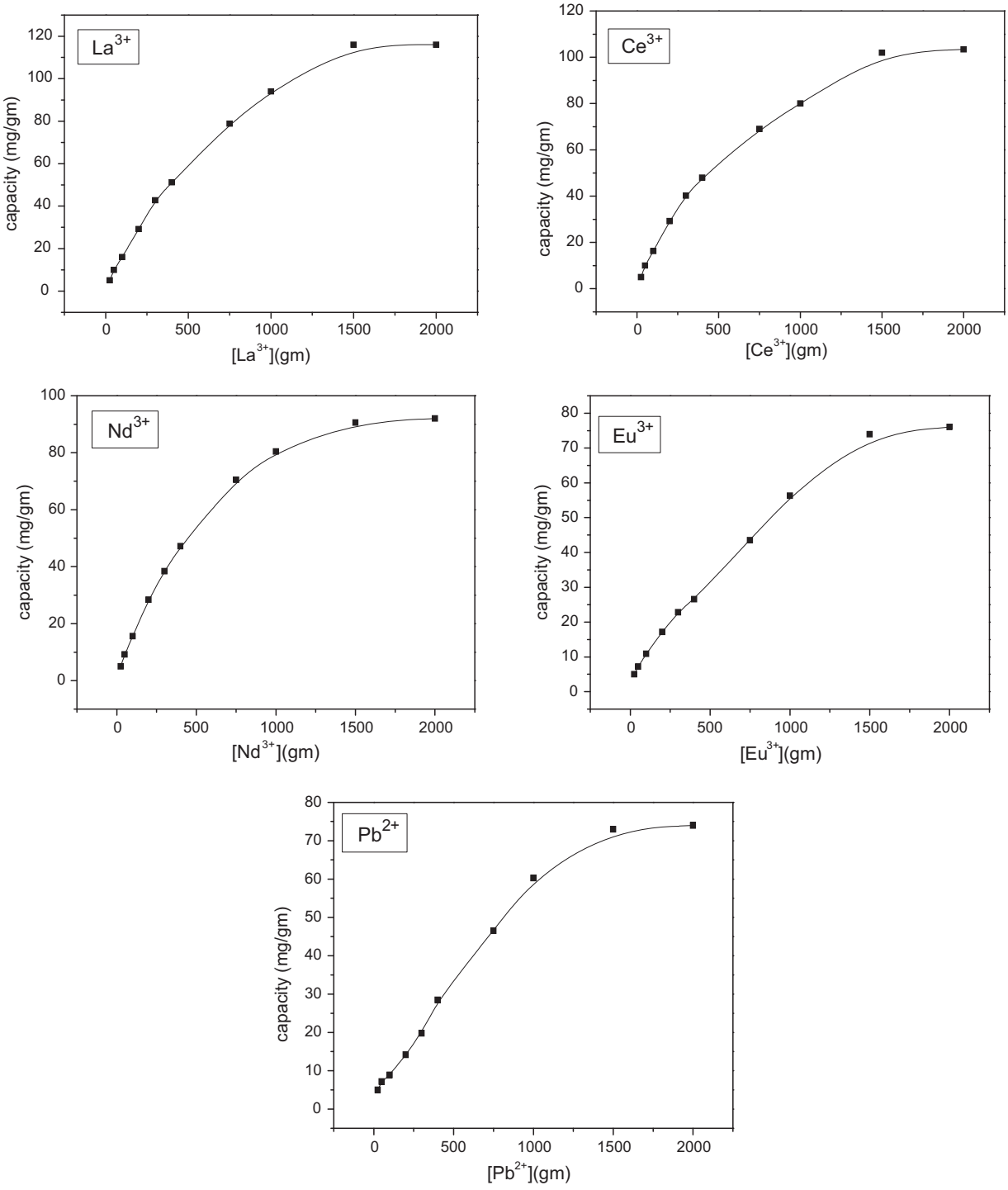


**Fig. 13.** Effect of initial metal ion concentration on the adsorption capacity of $La^{3+}$, $Ce^{3+}$, $Nd^{3+}$, $Eu^{3+}$ and $pb^{2+}$ onto P(VP-AMPS-$SiO_2$) composite.

*3.4.2.3. Effect of initial metal ions concentration on sorption of P(VP-AMPS-$SiO_2$) composites.* The initial concentration provides an important driving force to overcome all mass transfer resistance of metal ions between the aqueous and the solid phases. Batch experiments were also performed to study the effect of the initial metal ions concentration of $La^{3+}$, $Ce^{3+}$, $Nd^{3+}$, $Eu^{3+}$, $Pb^{2+}$ on their adsorption behavior on P(VP-AMPS-$SiO_2$) composite.

The adsorption process was carried out using 0.05 gm of the composite, 10 ml of each metal ion at different concentration ranged from 25 to 2000 mg/L, shaking time 3 h and at pH 4. The adsorption results show an initial rapid adsorption rate. As shown in Fig. 13(a–e), the maximum capacity of P(VP-AMPS-$SiO_2$) composite were found to be 116, 103, 92, 76 and 74 mg/g for $La^{3+}$, $Ce^{3+}$, $Nd^{3+}$, $Eu^{3+}$ and $Pb^{2+}$, respectively. It could be observed that the removal efficiency increases at lower initial concentrations because of sorption sites were easily occupied. However, as the initial concentration increases, most of sorption sites become occupied till it reached to full saturation.

According to these data it was found that the maximum capacity for P(VP-AMPS-$SiO_2$) composite toward metal's ion follows the order, $La^{3+} > Ce^{3+} > Nd^{3+} > Eu^{3+} > Pb^{2+}$. This order is in satisfactory agreement with the descending order of the crystal ionic radii. The observed trend of metal-ion uptake is correlated with the hydrated radii of the trivalent lanthanide ions; the relatively larger $Pb^{2+}$ ions are expected to pass slowly through voids on the surface, leading to relatively lower metal-ion capacity. One the other hand the basicity of metal's ion must be taken in consideration that arranged with the same order of decreasing basicity.

$La^{3+} > Ce^{3+} > Nd^{3+} > Eu^{3+}$.

## 4. Conclusion

P(VP-AMPS) hydrogel have been successfully prepared by radiation template polymerization of PVP, AMPS and DAM of concentration 0.5, 10 and 0.6 wt%, respectively, The percent conversion found to be 100% while, the swelling degree at the optimum condition was found to be 146 and the maximum capacity toward $Cu^{+2}$ metal ion reached to 91 mg/gm. Systematic preparation of P(VP-AMPS-$SiO_2$) composite were also achieved at silica concentration 0.3 wt% which, have a significantly higher sorption capacity toward Cu(II) reached to 99.8 mg/g due to highly crosslinked structure, as a result of the presence of silica. The prepared composite provided higher thermal stability than the prepared polymeric hydrogel. The obtained results revealed that the maximum capacity of P(VP-AMPS-$SiO_2$) composite was higher than the corresponding capacity of P(VP-AMPS) hydrogel. The maximum capacity reached to 116, 103, 92, 76, 74 mg/gm for $La^{3+}$, $Ce^{3+}$, $Nd^{3+}$, $Eu^{3+}$ and $Pb^{2+}$ respectively.

## References

[1] A.S. Gursel, L. Gubler, B. Gupta, G. Scherer, Radiation grafted membranes, Advances in Polymer Science Journal, Springer, Berlin, 2008, p. 215.
[2] B.Y. Ahn, S.I. Seok, I.C. Baek, J. Mater. Chem. 189 (2006).
[3] P. Mulvaney, P. Mulvaney, J. Angew. Chem. Int. Ed. 43 (40) (2004) 5393.
[4] A. Beganskiene, V. Sirutkaitis, M. Kurtinaitiene, Mater. Sci. 10 (4) (2004). ISSN 1392-1320.
[5] M. Darbandi, R. Thomann, T. Nann, J. Chem. Mater. 17 (23) (2005) 5720.
[6] J. Kameník, F. Sebesta, J. Phys. 56 (2006).
[7] A.A. El-Zahhara, H.M. Abdel-Aziza, T. Siyama, J. Macromol. Sci. Part A Pure Appl. Chem. 44 (2) (2007).
[8] K. Sukchola, S. Thongyaia, P. Praserthdam, J. Synth. Met. 179 (2013) P10–P17.
[9] R. Saito, J. Polym. 49 (11) (2008) 2625–2631.
[10] S.F. Abo-Zahra, PhD. Thesis, Faculty of Science, Ain Shams University, Cairo, Egypt, 2012.
[11] S. Dubinsky, G.S. Grader, G.E. Shter, M.S. Silverstein, J. Polym. Degrad. Stab. (2004) 171–178.
[12] M. Jithunsa, K. Tashiro, S. Chirachanchai, Int. J. Hydrogen Energy 36 (16) (2011) 10384–10391.
[13] K.F. Hassan, S.A. Kandil, H.M. Abdel-Aziz, T. Siyam, J. Chromatogr. Res. Int. (2011).
[14] A.D. Manita Jithunsa, B. Kohji Tashiro, C. Suzana Pereira Nunes, Suwabun Chirachanchai, Poly(acrylic acid-co-4-vinylimidazole)/sulfonated poly(ether ketone), 2010.
[15] S.C. Ghanshyam, G. Godawari, Department of Chemistry, Himachal Pradesh University, Shimla, India Study in Sorption of $Cr6^{+}$ and NO3 171005, 2008.
[16] W.H. Zhang, X.D. Fan, W. Tian, W.W. Fan, Express Polym. Lett. 6 (7) (2012) 532–542.
[17] H.D. Urrows, H.A. Ellis, S.I. Utah, Polymer 22 (1981) 1740.
[18] T. Siyam, Designed Monomers Polym. 4 (2001) 107.
[19] M.M. Senna, T. Siyam, S. Mahdy, J. Macromol. Sci. Part A Pure Appl. Chem. (2004) 1187–1203.
[20] K.A. Gschneidner, L. Eyring, Handbook on the Physics and Chemistry of Rare Earths, vol. P334, 2000, p. 28.
[21] S. Pereira, N. Kohji Tashiro, M. Jithunsa, Int. J. Hydrogen Energy (2011).